Uncoiling Mechanism of *Klebsiella pneumoniae* Type 3 Pili Measured by using Optical Tweezers

Feng-Jung Chen *[a,b], Chia-Han Chan [b], Kuo-Liang Liu [e], Ying-Jung Huang [b,c], Hwei-Ling Peng [c], Hwan-You Chang [d], Tri-Rung Yew [e], Ken Y. Hsu [a], and Long Hsu [b]

[a] Dept. of Photonics & Inst. of Electro-Optical Engineering, [b] Dept. of Electrophysics, [c] Dept. of Biological Science and Technology, National Chiao Tung University, 1001 Ta-Hsueh Road, Hsinchu, Taiwan 300, ROC

[d] Inst. of Molecular Medicine & Dept. of Life Sciences, [e] Dept. of Materials Science and Engineering, National Tsing Hua University, 101, Section 2, Kuang-Fu Road, Hsinchu, Taiwan 300, ROC

ABSTRACT

Pili are bacterial appendages that play many important roles in bacterial behaviors, physiology and interaction with hosts. Via pili, bacteria are able to adhere to, migrate onto, and colonize on host cells, mechanically. Different from the most studied type 1 and P type pili, which are rigid and thick with an average of 6~7 *nm* in diameter, type 3 pili are relatively tiny (3-5 *nm* in diameter) and flexible, and their biophysical properties remains unclear. By using optical tweezers, we found that the elongation processes of type 3 pili are divided into three phases: (1) elastic elongation, (2) uncoiling elongation, and (3) intrinsic elongation, separately. Besides, the uncoiling force of the recombinant pili displayed on the surface of *E. coli* [pmrkABCD$_{V1}$F] is measured 20 pN in average stronger than that of *E. coli* [pmrkABCD$_{V1}$]. This suggests that pilin MrkF is involved in determining the mechanical properties of the type 3 pili.

Keywords: Type 3 pili, Optical Tweezers, Mechanical properties, Uncoiling force

1. INTRODUCTION

Adherence to host cells is a critical step for a bacterium to establish successful infections. Most frequently, bacteria utilize tiny cell surface appendages called fimbial pili, which are typical 2-10 nm in diameter and 1-2 μm in length, to attach to certain surface molecules on host cells. Different pili can bind to different cell molecules and in turn result in distinct disease tropism [1, 2]. In general, mainly four types of pili are studied: type1, type 3, P type, and type 4.

Despite pili have been known for more than five decades, few studies have dealt with their mechanical properties presumably due to their small sizes. The improvement in the resolution of imaging techniques [3] and in the construction of force spectroscopes [15], such as atomic force microscopy (AFM), optical tweezers (OT), and so on, have gradually revealed the complicated protein-protein interactions for pilus assembly and how a pilus is organized .

Recently, the active force of a single type 4 pilus motor has been measured by using OT [4-5]. Besides, some passively mechanical properties, such as three phases of elongation behavior, of type 1 and P type pili have also been quantitatively characterized by OT [6-7] or AFM [8-9]. These nanotechnologies are already advancing our understanding of pilus physiology, adhesion properties, and assembly events, while providing new opportunities to probe the dynamic and physical aspects of molecules and delicate quantitative measurement. However, different from the most studied type 1 and P type pili, the biophysical properties of type 3 pili remains unclear.

Type 3 pili are unique to *Klebsiella pneumoniae*, which is an opportunistic pathogen with high prevalent rates in Taiwan, and share low sequence homology with P type pili and type 1 pili. Moreover, type 3 pili have been strongly implicated as a virulence factor [10-11]. Thus, the elucidation of assembly mechanism of this kind of pili may aid in developing therapeutic agents to prevent the bacteria infection.

Recently, the nucleotide sequences of six genes involved in the expression of type 3 pili of *Klebsiella pneumoniae* were identified [12]. Those genes are *mrk*A, *mrk*B, *mrk*C, *mrk*D, *mrk*E, and *mrk*F. First of all, *mrk*A gene encodes the major fimbrial subunit. Second, *mrk*B and *mrk*C are membrane-associated genes. Third, *mrk*D gene encodes *Klebsiella*-like

Optical Trapping and Optical Micromanipulation IV, edited by Kishan Dholakia, Gabriel C. Spalding,
Proc. of SPIE Vol. 6644, 66441W, (2007) · 0277-786X/07/$18 · doi: 10.1117/12.733097

hemagglutinin-specific adhesin activity. Forth, *mrk*E genes appear involved in the regulation of type 3 fimbrial expression. Finally, *mrk*F gene product is required to maintain the stability of type 3 pili on the bacterial surface via qualitative measurements. However, the mechanical properties due to intermolecular attraction between major subunits, MrkA proteins, were not clear; likewise, the quantitative stabilities of the type 3 pili with or without *mrk*F were not demonstrated.

In this study, we will measure the mechanically elongation behavior of type 3 pili by used optical tweezers [13-15]. Besides, we will quantitatively analyze the functions of *mrk*F genes in terms of mechanical properties of type 3 pili.

2. MATERIALS AND METHOD

2.1 Bacterial Strains and Beads' Functionalization

Type 3 pili of *K. pneumonia*e were displayed on the surface of *E. coli* JM109, a non-type 3 pili-producing strain, by transformation of a plasmid carrying *mrk* operon with or without *mrk*F gene. The plasmids used in the study include [pmrkABCD$_{V1}$] and [pmrkABCD$_{V1}$F]. Prior to the force-versus-elongation measurement, the *E. coli* transformants were grown in LB medium (with 100 μm/ml ampicillin antibiotics) at 37^{o}C for 20 hours to generate lower density distribution of type 3 pili upon the surface of a bacterium [16].

1 μm carboxyl latex beads (Polysciences, Inc. Warrington, PA, USA) were functionalized with 1-ethyl-3-(3-dimethylaminopropyl) carbodiimide hydrochloride (EDAC) and N-hydroxysuccinimide (NHS) for a study of a force-versus-elongation measurement of type 3 pili [17]. In brief, the beads were washed in 0.025 M MES buffer, pH6.0. To activate the beads, the beads were resuspended in 1.0 ml of activation buffer (0.1 M MES, 0.5 M NaCl, and pH5.0). EDAC (0.4 mg) and NHS (0.6 mg) were added to the suspension and incubated at room temperature for 20-30 min. Beads were washed, resuspended in 50 μl activation buffer, and stored at 4^{o}C to be used within 1 day of preparation. However, in this study the beads functioned as a surface onto which pili could bind non-specifically through the inherent hydrophobicity of the bead. This functionalization, which is described elsewhere [6], is therefore believed not to have any influence on the study of the mechanical properties of a single type 3 pilus presented in this work.

In addition to the beads' functionalization, glass coverslips were washed thoroughly, cleaned completely. Just before use, the coverslips were dried and placed into a holder.

2.2 Optical Tweezers Systems

A fiber laser (10W, single-mode cw, 1064 nm, YLR-10-1064, IPG, USA) was used as the trapping laser beam of our optical tweezers system. The trapping beam was guided into an inverted microscope (DMIRB, Leica, Germany) with a high numerical aperture objective (100× oil, NA=1.25, NPLAN, Leica, Germany). Furthermore, the specimen holder of the sample was mounted on a PZT stage (P-611.XZS, PI, Germany) with a minimum step size of 2 nm and a maximum travel range of 100 μm during its closed operation.

The basic principle of the trapping force of the optical tweezers technique can be briefly described as follows. The trapping force on a small spherical bead in a trap created by optical tweezers is linearly proportional to the position of the bead in the trap as the displacement is less than half the radius of the bead [18]. A small particle held by the optical tweezers will therefore shift its position in the trap an amount that is proportional to any external force to which it is exposed. Therefore, the force exerted onto a trapped bead at any moment in time can thereby be determined by monitoring the displacement of the bead in the trap.

The position of a small spherical bead in the trap can conveniently be monitored by the use of a probe laser, which in our system was a stabilized HeNe laser (0.5mW, 1507-1, JDS Uniphase, USA) with lower intensity than the trapping power to prevent interference with the balance of forces in the system. The probe beam is off-focused below the trapped bead in such a way that the bead scatters the light to a distinct spot in the far field and the forward scattering pattern of the collected light on the back focal plane of the condenser (20×, NA=0.5, Plan Fluor, Nikon, Japan) was imaged on a quadrant-photodiode (QPD, S5981, Hamamatsu, Japan). The voltage signals output from the QPD are processed via a preamplifier and then a main amplifier (Öffner, MSR-Technik, Germany) with a amplification factor of 10 and a cut-off frequency of 1 MHz. Subsequently, a DAQ card (NI-6115, NI, USA) was used to record the voltage signals with a sampling rate of 200 kHz for a simultaneous acquisition of three channels.

A bright-field illumination was achieved by using a halogen lamp through a lens and the condenser. The images wee taken by using a CCD camera (12v1E, Mirtron, Taiwan) with a filter blocking the unwanted laser light (shown in Fig. 1).

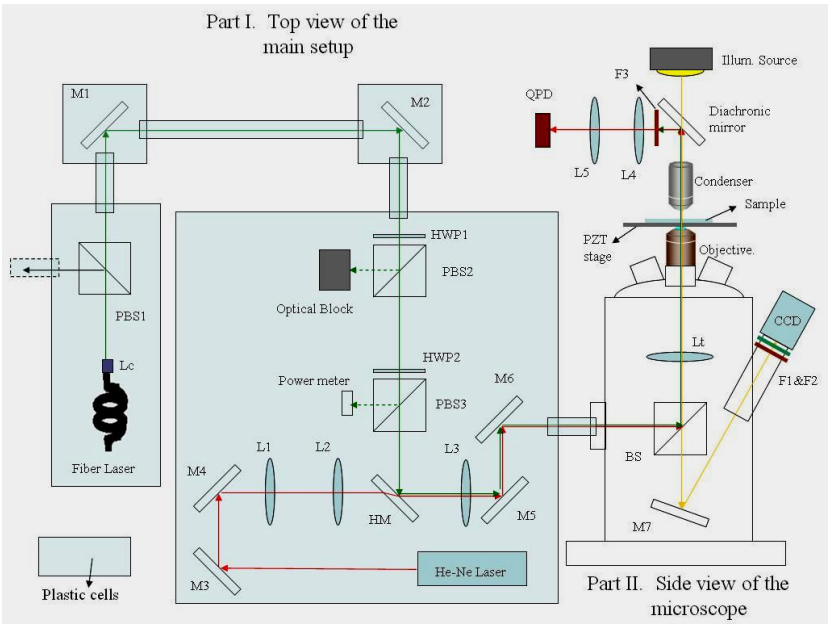

Fig. 1. Simplified schematic of the optical tweezers system (not to scale). The near-infrared laser (fiber laser) was used as the optical trapping beam. The laser power is controlled via a rotatable halfwave plate (HWP2), automatically controlled via a computer, and polarizing beam splitter (PBS3) and detected by a power meter (818-SL, Newport, USA). After the polarizer, the beam is expanded to slightly overfill the back pupil of the high numerical objective. The He-Ne laser was used as the probing beam. The lasers were together guided into the epiillumination path of an inverted microscope and reflected by a dichroic mirror into the objective. The laser lights was focused by the objective to form a trap in the specimen plane and the forward scattering pattern of the collected light on the back focal plane of the condenser was imaged on a quadrant-photodiode. The illuminating light passes through the dichroic mirror to a video camera (CCD).

2.3 Calibration Procedures

Before each measurement, the stiffness of the optical trap (defined as the derivate of the force with respect to distance for a small particle in the trap) was assessed using a calibration technique based upon the power spectrum of the Brownian motion of the trapped particle [19]. The main advantage of this technique is that can be performed rapidly in situ; a typical calibration procedure takes only a 10 seconds. A calibration can therefore be done before each measurement. To validate the Brownian motion calibration technique, separate calibrations were performed based upon the mean square value of the position of the trapped particle. The two calibration techniques were found to concur to within a few percent.

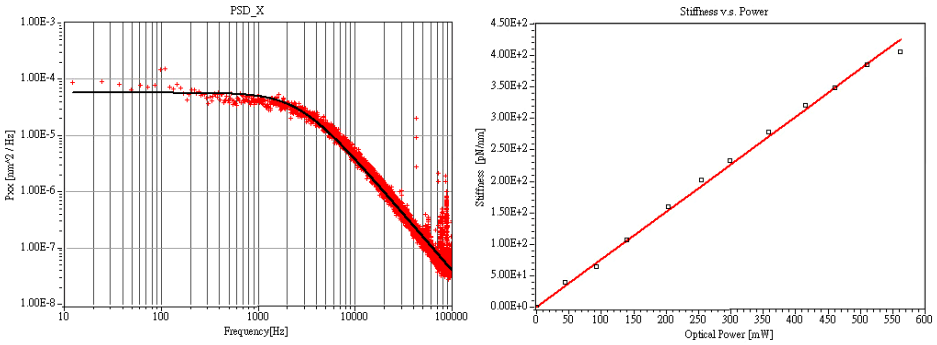

Fig. 2. A) Power spectrum of a 1 μm diameter polystyrene bead was held in the laser trap with a corner frequency f_c = 3423.49 ± 6 Hz. The power spectrum shown is the average of 60 independent power spectra. It consists of a thermal background caused by Brownian motion. The sampling frequency was f_{sample} = 65,536 Hz, the measurement time for each spectrum was 5 s, and the temperature was 26 °C. B) Stiffness of the trap-verser-output power. The good linearity illustrates both that the system has no severe misalignments and that the fiber laser has good intensity stability.

Typical stiffness values of the optical trap in our system were in the 0.040-0.405 pN/nm range, which corresponded to a laser power of from 44 mW to 560 mW measured directly at the sample (shown in Fig. 2(B)). The separation velocity for the measurements reported here was 0.5 μm/s. This implied that the loading rates were in the range between 5 and 200 pN/s.

2.4 Force Measured Procedures

Samples were prepared directly on the cleared coverslip by sequentially adding 40 μl freshly resuspended *E. coli* in PBS. Another coverslip was placed on top separated by a two layers of double-slide tapes onto the microscope and incubated for 20-30 min to valid the bound between bacteria and the lower coverslip. Then, the PBS with unbound *E. coli* was sucked and immediately 40 μl activated1.0-μm beads were added into the sample.

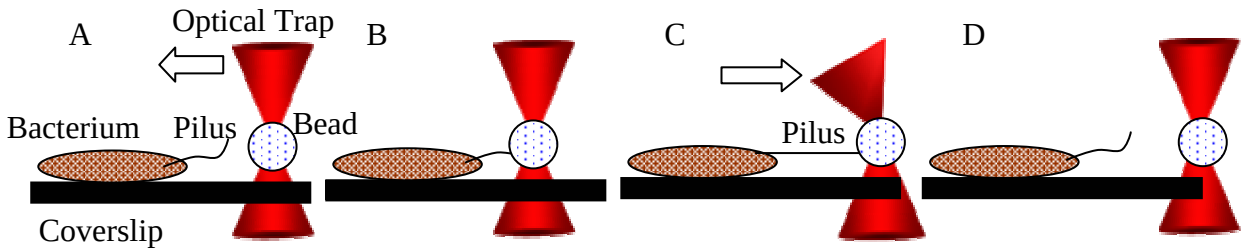

Fig. 3. Force measured procedures. (A) A bacterium is mounted upon a coverslip. The trapped bead serves as a force indicator in the optical tweezers system and is moved to approach a single pilus. (B) A strong bond is formed between the trapped bead and the bacterial pili. (C) A force is exerted on the pili by moving the coverslip. (D) The pilus detached from the bound bead.

Next, a suspended bead was trapped by the optical tweezers. The trap was then calibrated before the bead and moved the bead to approach a bacterium, which was attached on the under coverslip, but not to touch a bacterial surface. Then a probably automatic formation of an attachment between a pilus and a bead was waited for few seconds. Furthermore, to confirm the formation of an attachment, attempts were made to slightly separate the bead and the bacterium.

Finally, Move a coverslide by a piezo-stage to gradually separate the bead and the pilus. A force could be exerted on the pilus bound to the bead. As the force was increased, the position of the bead became displaced a small distance relative the center of the trap. Then the position of the bead was therefore continuously monitored until the elongation behavior of the pilus, providing continuous information of the force variation as a function of position of the coverslip, which in turn could be related to the length of the pilus (shown in Fig. 3).

2.5 Transmission Electron Microscopy (TEM) Images

First, the *E. coli* JM109 [pmrkABCD$_{V1}$F] and [pmrkABCD$_{V1}$] incubated for 16 hours [16]. Next, these *E. coli* were negatively stained with 2% phosphotungstic acid (PTA) on a formvar/carcon copper-grid [20]. Finally, the sample were subsequently sealed and putted in TEM (JEM-2010, JEOL) with operated voltage of 200 kV to observe.

3. RESULTS

3.1 The structure of type 3 pili

In order to study the dependence of the elongation of a single type 3 pilus as a function of the stretching force exerted by optical tweezers, we have prepared a strain of *E. coli* transformants, grown in LB medium, which expresses the desired type 3 pili of low density. Fig. 4(A) shows the TEM image of an *E. coli* with only a few pili: typically, 15 pili per bacterium. As shown in Fig. 4(B), the pili are of approximately l = 2 μm in length and D = 3.6 nm in diameter. With this strain of *E. coli*, it is feasible for us to adhere to a single type 3 pilus and then to perform the force-versus-elongation measurement by using optical tweezers.

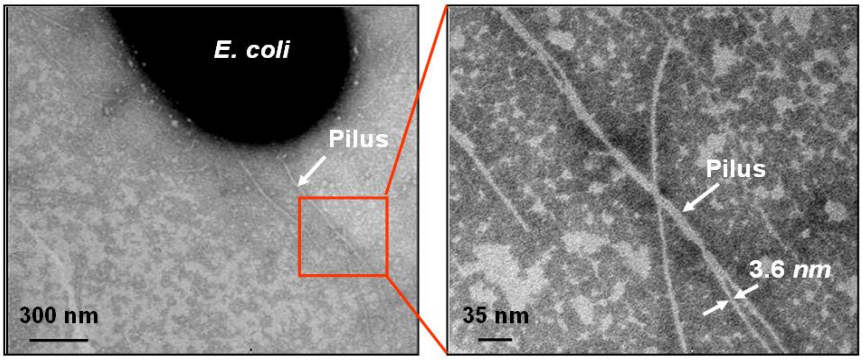

Fig. 4. A) TEM images of E. *coli* JB109 with [pmrkABCD$_{V1}$F]. Type 3 pili are in average 3.6 nm in diameter and ~2 μm in length. An *E. coli* is with only a few pili; typically, 15 pili per bacterium. B) It is locally enlarged image of the image in A).

3.2 Three phases of elongation behaviors of a type 3 pilus

Fig. 5 shows that the elongation of type 3 pili can be classified into three phases: namely, (1) elastic elongation, (2) uncoiling elongation, and (3) intrinsic elongation, separately. It is obvious to see that, in the elastic phase, a type 3 pilus first elongates linearly with the increasing stretching force like a coil for weak stretching force. As the stretching force reaches around 85 pN, the elongation behavior of the pilus switches dramatically from the elastic phase into the uncoiling phase. In this peculiar phase, the fully stretched pilus, a rod of a helical structure of MrkA, keeps elongating at the fixed stretching force of 85 pN by uncoiling their helical structure one turn by another. Eventually, the length of the completely uncoiled pilus would be twice as long as its original length at the end of the uncoiling phase. As the stretching force keeps increasing, the further elongation of the completely uncoiled pilus shifts into the intrinsic phase. In the final intrinsic phase, the elongation of the pilus is nonlinear with the increasing force, which is believed an overstretching of the completely uncoiled structure.

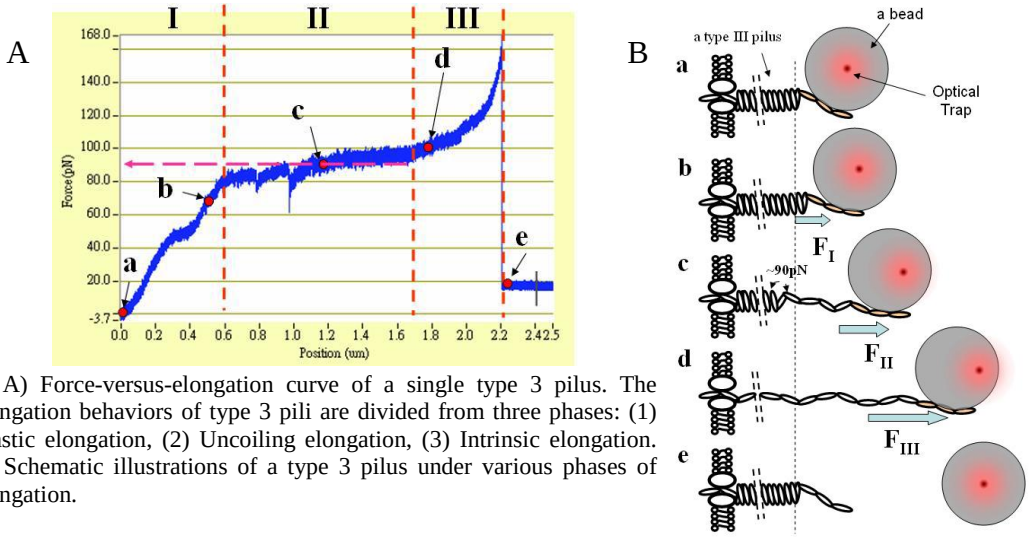

Fig. 5. A) Force-versus-elongation curve of a single type 3 pilus. The elongation behaviors of type 3 pili are divided from three phases: (1) Elastic elongation, (2) Uncoiling elongation, (3) Intrinsic elongation. B) Schematic illustrations of a type 3 pilus under various phases of elongation.

In the elastic phase in Fig. 5(A), the mechanical property of the type 3 pilus can be characterized by the traditional elasticity modulus, which is also called *Young*'s modulus

$$E = \frac{F/A}{\Delta l / l} = \frac{k_p}{\pi (D/2)^2 \times l}, \quad (1)$$

in which F (in units of N) is the stretching force to the pilus, A (in units of m^2) = $\pi (D/2)^2$ is the cross area of the pilus, D (in units of m) is the diameter of the pilus, l (in units of m) is the original length of the pilus, Δl (in units of m) is the elongated length of the pilus, and k_p (in units of N/m) is the stiffness of the pilus. Note that the stiffness k_p of the type 3 pilus is simply the slope of elongation-force curve in this phase: accordingly, $k_p \cong 0.219$ pN/nm. Consequently, substituting 0.219 pN/nm, 12 μm, and 3.6 nm into Eq. (1) for k_p, l, and Δl, respectively, results in a *Young*'s modulus of 10.75 MPa (in units of pN/μm^2). This suggests that the elongation behavior of type 3 pili in the elastic phase is similar to that of rubber.

In the uncoiling phase in Fig. 5(A), like type 1 or P type pili, type 3 pili also reveal a plateau phase in the force-versus-elongation curve. Similarly, we believe that this behavior results from the uncoiling of the helical (quaternary) structure of MrkA in a serial manner at a constant force [6]. This signature confirms that the elongation of the pili and the corresponding binding pili are no longer elastic as the uncoiling process begins. Once the helical structure of the pilus has been completely uncoiled and turned into a chain, as shown in Fig. 5(B), larger and larger forces are required to keep stretching the chain.

Subsequently, in the intrinsic phase in Fig. 5(c), the slope of the elongation-force curve becomes steeper and steeper as the stretching force increases. The details of this behavior remain unclear yet. However, at the end of the nonlinear elongation in this phase, a sudden drop of the stretching force occurs. This force is referred to the rupture force due to the detachment of the pilus from the bound bead.

3.3 The mechanical properties of type 3 pilus with *mrk*F and without *mrk*F

As to the function of gene *mrkF*, only one paper was found related to the stability of type 3 pili containing *mrk*F [12] up to now. Qualitatively, this paper mentioned that it is easier for type 3 pili without *mrk*F than those with *mrk*F to detach from the surface of *E. coli* when the environmental temperature exceeds 55°C. However, there is no quantitative comparison between their mechanical properties otherwise. In this study, we found that the uncoiling force of the recombinant pili displayed on the surface of *E. coli* [pmrkABCD$_{V1}$F] is measured 20 pN in average stronger than that of *E. coli* [pmrkABCD$_{V1}$], as shown in Fig. 6. This suggests that gene *mrk*F is involved in determining the mechanical properties of the type 3 pili.

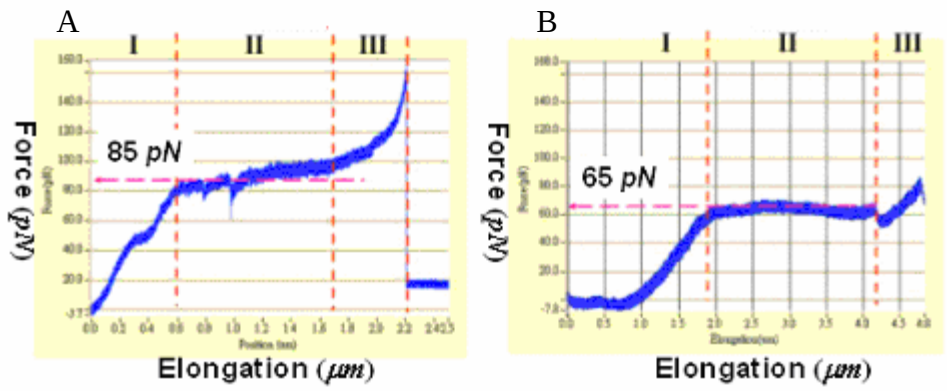

Fig. 6. A) Force-versus-elongation curve of a single type 3 pilus in present of *mrk*F gene. The uncoiling force is 85 pN. B) Force-versus-elongation curve of a single type 3 pilus in absence of *mrk*F gene. The uncoiling force is 65 pN. This suggests that *mrk*F is involved in determining the mechanical properties of the type 3 pili

4. CONCULSION

We have employed optical tweezers technique to investigate the three phases of elongation behaviors of type 3 pili: (1) elastic elongation, (2) uncoiling elongation, and (3) intrinsic elongation. Firstly, in the elastic phase, the *Young*'s modulus of type 3 pili is estimated to be 10.75 MPa. This suggests that type 3 pili are similar to rubber in terms of mechanical property under weak stretching force. Next, in the uncoiling phase, the uncoiling force of type 3 pili is approximately 85pN, which is larger than those of P type pili and type 1 pili. This suggests that type 3 pili have a stronger interaction between adjacent turns of the helical rod. Lastly, in the intrinsic phase, the elongation behavior is nonlinear. This suggests that a larger force is then required to stretch the chain-like pilus after the rod has been completely uncoiled.

In addition to the elongation behavior of type 3 pili, we have also quantitatively measured that *E. coli* [pmrkABCD$_{V1}$F] is 20 pN in average stronger than that of *E. coli* [pmrkABCD$_{V1}$]. This suggests that gene *mrk*F is involved in determining the mechanical properties of type 3 pili.

We hope that this study provides new insights to understand the physiological mechanism of bacteria in resisting the shear flow in human body [21].

5. ACKNOWLEDGEMENT

This work is supported by research grants from the National Science Council and the National Chiao Tung University, Taiwan. Furthermore, we thank Professor Cheng-Hsien Liu, Dept. Power Mechanical Engineering, National Tsing Hua Univ., Taiwan, for helpfully technical discussion.

REFERENCES

1. Esther Bullitt and Lee Makowski, "Structural polymorphism of bacterial adhesion pili," *Nature* 373, 164-167 (1995).
2. Sauer FG, Barnhart M, Choudhury D, Knight SD, Waksman G, and Hultgren SJ, "Chaperone-assisted pilus assembly and bacterial attachment," *Curr. Opin. Struct. Biol.* 10, 548-556 (2000).
3. Xiang-Qi Mu and Esther Bullitt, "Structure and assembly of P-pili: A protruding hinge region used for assembly of a bacterial adhesion filament," *Proc. Natl. Acad. Sci. USA.* 103, 9861-9866 (2006).
4. Alexey J. Merz, Magdalene So and Michael P. Sheetz, "Pilus retraction powers bacterial twitching motility," *Nature* 407, 98-102 (2000).
5. Berenike Maier, Laura Potter, Magdalene So, Hank S. Seifert, and Michael P. Sheetz, "Single pilus motor forces exceed 100 pN," *Proc. Natl. Acad. Sci. USA.* 99, 16012-16017 (2002).
6. Jana Jass, Staffan Schedin, Erik Fallman, Jorgen Ohlsson, Ulf J. Nilsson, Bernt Eric Uhlin, and Ove Axner, "Physical Properties of *Escherichia col*i P Pili Measured by Optical Tweezers," *Biophys. J.* 87, 4271-4283 (2004).
7. Erik Fallman, Staffan Schedin, Jana Jass, Bernt-Eric Uhlin, and Ove Axner, "The unfolding of the P pili quaternary structure by stretching is reversible, not plastic," *EMBO Report* 6, 1-5 (2005).
8. Eric Miller, Tzintzuni Garcia, Scott Hultgren, and Andres F. Oberhauser, "The Mechanical Properties of *E. coli* Type 1 Pili Measured by Atomic Force Microscopy Techniques," *Biophys. J.* 91, 3848-3856 (2006).
9. Manu Forero, Olga Yakovenko, Evgeni V. Sokurenko, Wendy E. Thomas, and Viola Vogel, "Uncoiling Mechanics of *Escherichia coli* Type I Fimbriae Are Optimized for Catch Bonds," *PLos Bio.* 4, 1509-1516 (2006).
10. Ann-Mari Tarkkanen, Ritva Virkola, Steven Clegg, and Timo K. Korhonen, "Binding of the Type 3 Fimbriae of *Klebsiella pneumoniae* to Human Endothelial and Urinary Bladder Cells," *Infection and Immunity* 65, 1546-1549 (1997).
11. Patrick Di Martino, Nathalie Cafferini, Bernard Joly and Arlette Darfeuille-Michaud, "*Klebsiella pneumoniae* type 3 pili facilitate adherence and biofilm formation on abiotic surfaces," *Research in Microbiology* 154, 9-16 (2003).
12. Bradley L. Allen, Gerald-F. Gerlach, and Steven Clegg, "Nucleotide Sequence and Functions of mrk Determinants Necessary for Expression of Type 3 Fimbriae in *Klebsiella pneumoniae*," *Journal of Bacteriology* 173, 916-920 (1991).
13. A. Ashkin, J. M. Dziedzic, J. E. Bjorkholm, and Steven Chu, "Observation of a single-beam gradient force optical trap for dielectric particles," *Optics Letters* 11, 288-290 (1986).
14. Keir C. Neuman and Steven M. Block, "Optical trapping," *Review of Scientific Instruments* 75, 2787-2809 (2004).

15. William J. Greenleaf, Michael T. Woodside, and Steven M. Block, "High-Resolution, Single-Molecule Measurements of Biomolecular Motion," *Annu. Rev. Biophys. Biomol. Struct.* 36, 171-190 (2007).
16. Y.-J. Huang, C.-C. Wu, M.-C. Chen, C.-P. Fung, and H.-L. Peng, "Characterization of the type 3 fimbriae with different MrkD adhesins: Possible role of the MrkD containing an RGD motif," *Biochemical and Biophysical Research Communications* 350, 537-542 (2006).
17. Staros, J. V., R. W. Wright, and D. M. Swingle. "Enhancement by N-hydroxysulfosuccinimide of water-soluble carbodiimide-mediated coupling reactions," *Anal. Biochem.* 156, 220–222 (1986).
18. A. Ashkin, "Forces of a single-beam gradient laser trap on a dielectric sphere in the ray optics regime," *Biophys. J.* 61, 569-582 (1992).
19. Kirstine Berg-Sørensen and Henrik Flyvbjerg, "Power spectrum analysis for optical tweezers," *Review of Scientific Instruments* 75, 594-612 (2004).
20. Xiaohong Huang and Qiya Zhang, "Improvement and observation of immunoelectron microscopic method for the localization of frog Rana grylio virus (RGV) in infected fish cells," *Micron* 38, 599-606 (2007).
21. Thomas, W. E., L. M. Nilsson, M. Forero, E. V. Sokurenko, and V. Vogel, "Shear-dependent 'stick-and-roll' adhesion of type 1 fimbriated *Escherichia coli*.," *Mol. Microbiol.* 53, 1545-1557 (2004).